

**[5]Trovacenyl Boronic Acid, (η^7 -C₇H₇)V[η^5 -C₅H₄B(OH)₂],
and Its Anhydride Tri([5]trovacenyl)boroxine,
1,3,5-[(η^7 -C₇H₇)V(η^5 -C₅H₄)]₃B₃O₃ †,1**

Christoph Elschenbroich,* Matthias Wolf, Jürgen Pebler, and Klaus Harms

Fachbereich Chemie der Philipps-Universität, D-35032 Marburg, Germany

Received August 12, 2003

The paramagnetic boronic acid (η^7 -C₇H₇)V[η^5 -C₅H₄B(OH)₂] (**3**[•]) has been prepared and characterized structurally, emphasis being placed on hydrogen bonding motives present in the crystal. EPR spectroscopy reveals that association of **3**[•] is absent in fluid solution. Tri-([5]trovacenyl)boroxine, **4**^{•••}, the cyclic anhydride of **3**[•], engages in antiferromagnetic exchange; magnetic susceptometry provides the value $J(\mathbf{4}^{\bullet\bullet\bullet}) = -1.04 \text{ cm}^{-1}$. Accordingly, the EPR spectrum of **4**^{•••} in fluid solution points to 22 ⁵¹V hyperfine components separated by one-third of the coupling constant of mononuclear trovacene derivatives. Redox splittings $\delta E_{1/2}$ between consecutive oxidation steps of **4**^{•••} are not resolved, i.e., $\delta E_{1/2} \leq 60 \text{ mV}$.

Introduction

Boronic acids, due to their ability to engage in metal-catalyzed cross-coupling reactions, have become highly valuable reagents in organic synthesis.² The extensive list of synthons also includes ferrocenyl boronic acids.³ Our occupation with the unsymmetrical paramagnetic sandwich complex (η^7 -C₇H₇)V(η^5 -C₅H₅) (trovacene, **1**[•]) triggered the synthesis of [5]trovacenyl boronic acid (η^7 -C₇H₇)V[η^5 -C₅H₄B(OH)₂] (**3**[•]), which is reported herein.⁴ Our interest in **3**[•] derives from questions relating to hydrogen bonding and from its use in the synthesis of oligonuclear trovacene derivatives, the simplest of them being the cyclic anhydride tris([5]trovacenyl)boroxine, 1,3,5-[(η^7 -C₇H₇)V(η^5 -C₅H₄)]₃B₃O₃ (**4**^{•••}). Conceivable hydrogen-bonded aggregates (**3**[•])_n as well as the cyclic anhydride **4**^{•••} invite studies of intramolecular electron–electron spin–spin interaction (“exchange coupling”) similar to those performed by us previously on [5]trovacenyl carboxylic acid, [(η^7 -C₇H₇)V(η^5 -C₅H₄COOH)]₂ (**6**[•])₂,⁵ and tris([5]trovacenyl)borane, [(η^7 -C₇H₇)V(η^5 -C₅H₄)]₃B (**7**^{•••}).⁶ In a more general vein, the ability of boronic acids to form complexes with diols⁷ suggests applications of **3**[•] that profit from the paramagnetic nature of trovacene such as studies of the transport of trovacenylboronl carbohydrate complexes.⁸

Results and Discussion

Lithiation of trovacene (**1**[•]), subsequent reaction with tributylborate to form ([5]trovacenyl)dibutylborate (**2**[•]), and hydrolysis afford [5]trovacenyl boronic acid (**3**[•]), which readily forms the cyclic anhydride tris([5]trovacenyl)boroxine (**4**^{•••}) upon heating in vacuo or by chemical means (Scheme 1). The cyclic ester **5**[•], which may be advantageous in C–C coupling reactions, is formed by reacting **3**[•] with ethylene glycol. The boronic acid **3**[•] is soluble in polar and aromatic organic solvents and sparingly soluble in water. **3**[•] may be extracted with aqueous base, however, which serves to effect separation from unreacted trovacene. Whereas from solvents that are inept to participate in hydrogen bonding **3**[•] could be obtained only as an amorphous powder, crystals suitable for X-ray diffraction can be grown from aqueous solution or from wet diethyl ether in the form of the adducts **3**[•]·H₂O and **3**[•]·Et₂O, respectively.

X-ray Crystallography. The structures of the adducts **3**[•]·Et₂O and **3**[•]·H₂O in the crystal are displayed in Figures 1 and 2, and selected bond lengths and angles are given in the captions. For the purpose of comparison, a glance at the structure of phenylboronic acid, C₆H₅B(OH)₂ (**8**),⁹ may be in order: two independent molecules of **8** are linked by a pair of O–H···O hydrogen bonds, the resulting dimeric units being hydrogen-bonded to four other units of the same kind. An infinite array of stacked layers is created thereby. The more bulky trovacenyl group prevents adoption of a similar layer structure by **3**[•]. Instead, packings are realized in which the hydrogen-bonding capacity of the –B(OH)₂ group is not used fully for association of the [5]trovacenyl boronic acid molecules themselves. Rather one OH group in **3**[•]·Et₂O and both OH groups in **3**[•]·H₂O directly hydrogen bond to the respective solvent molecule present

* To whom correspondence should be addressed. E-mail: eb@chemie.uni-marburg.de.

† Dedicated to Professor Werner Massa on the occasion of his 60th birthday.

(1) Trovacene Chemistry. 7. Part 6: Elschenbroich, Ch.; Plackmeyer, J.; Harms, K.; Burghaus, O.; Pebler, J. *Organometallics* **2003**, *22*, 3367.

(2) (a) Miyaura, N.; Suzuki, A. *Chem. Rev.* **1995**, *95*, 2457. (b) Miyaura, N. *Top. Curr. Chem.* **2002**, *219*, 11.

(3) (a) Nesmeyanov, A. N.; Ssasonova, V. A.; Drozd, V. N. *Chem. Ber.* **1960**, *93*, 2717. (b) Shechter, H.; Helling, J. F. *J. Org. Chem.* **1961**, *26*, 1034. (c) Knapp, R.; Rehan, M. *J. Organomet. Chem.* **1993**, *452*, 235. (d) Braga, D.; Polito, M.; Braccacini, M.; D'Addario, M.; Tagliavini, E.; Sturba, L. I.; Grepioni, F. *Organometallics* **2003**, *22*, 2142.

(4) Wolf, M. Ph.D. Thesis, Marburg, Germany, 1998.

(5) Elschenbroich, Ch.; Schiemann, O.; Burghaus, O.; Harms, K. *J. Am. Chem. Soc.* **1997**, *119*, 7452.

(6) Elschenbroich, Ch.; Wolf, M.; Burghaus, O.; Harms, K.; Pebler, J. *Eur. J. Inorg. Chem.* **1999**, 2173.

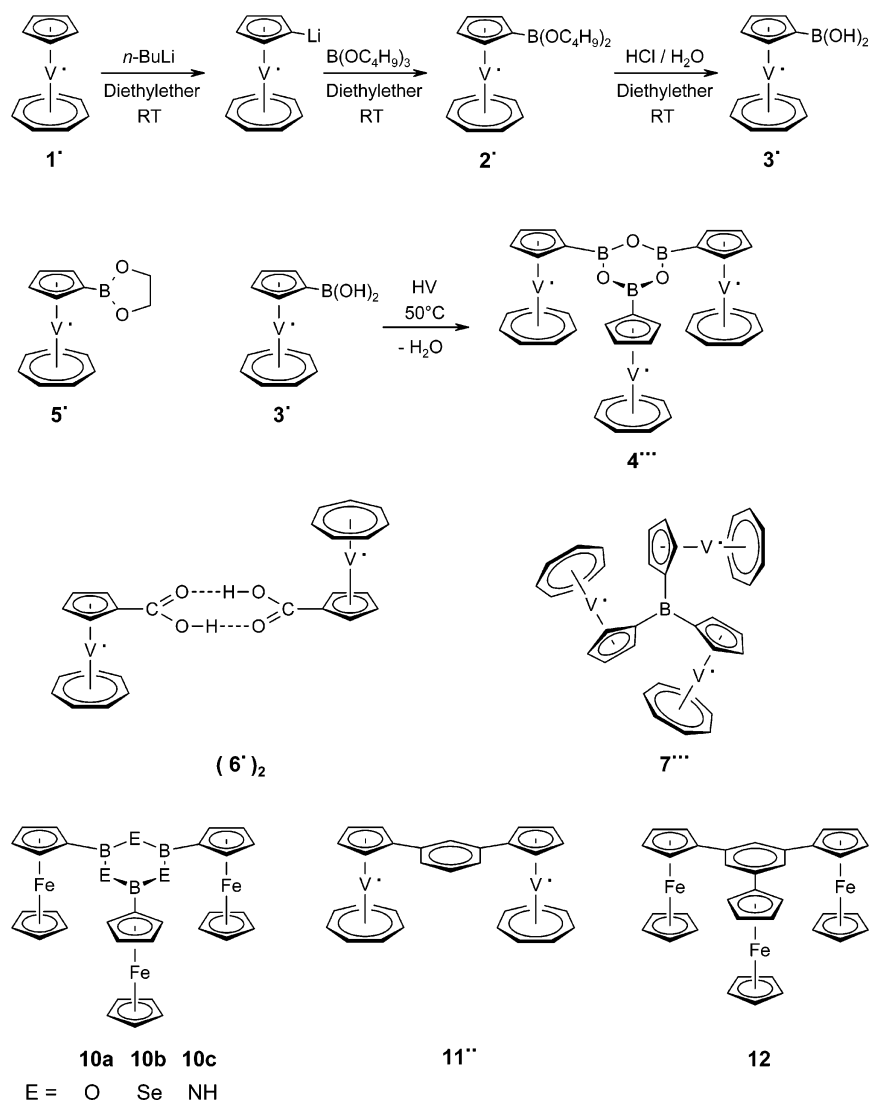
(7) (a) Lorand, J. P.; Edwards, J. O. *J. Org. Chem.* **1959**, *24*, 769.

(b) Norrild, J. C.; Eggert, H. *J. Am. Chem. Soc.* **1995**, *117*, 1479.

(8) (a) Morin, G. T.; Huglies, M. P.; Pangam, M.; Smith, B. D. *J. Am. Chem. Soc.* **1994**, *116*, 8895. (b) Pangam, M.; Valencia, L. S.; Boggess, B.; Smith, B. D. *J. Am. Chem. Soc.* **1994**, *116*, 11203. (c) Westmark, P. R.; Smith, B. D. *J. Am. Chem. Soc.* **1994**, *116*, 9343.

(9) Rettig, S. J.; Trotter, J. *Can. J. Chem.* **1977**, *55*, 3071.

Scheme 1



in the crystal lattice. Accordingly, in the structure of $3 \cdot \text{Et}_2\text{O}$ strings of the type $(\cdots\text{O}_\text{H}-\text{B}-\text{O}-\text{H}\cdots)_n$ are encountered in which the hydrogen atom not part of the chain hydrogen binds to Et_2O . The trovacenyl groups are connected to the boron atoms in alternating orientations whereby the sandwich axes assume angles of 90° . Thus, whereas the hydrogen-bonded chains in ferrocenyl diboronic acid $[\eta^5\text{-C}_5\text{H}_4\text{B}(\text{OH})_2]_2\text{Fe}$ (**9**) crisscross in the crystal structure,^{3d} in $3 \cdot \text{Et}_2\text{O}$ they are unidirectional.

In line with this disposition, two markedly different hydrogen bonds are observed: The hydrogen bond $\text{O}(1)-\text{H}(1)\cdots\text{O}(2)$ (76.0, 224.0 pm; 169.4°), which is part of the string, is slightly longer than that found in phenyl boronic acid **8** (79.0, 196.0 pm; 176°),⁹ in accordance with the lower Brønsted acidity of **3*** compared to **8**, trovacenyl being a stronger electron donor than phenyl. The parameters of the hydrogen bond $\text{O}(2)-\text{H}(2)\cdots\text{O}(3)$ (80.0, 199.0 pm; 170.4°), which connects one OH group to the ether molecule, is more similar to that in **8**. The structural features of the trovacene unit in **3** are unexceptional; they mimic those found for the parent complex **1**.¹⁰

The hydrogen atom positions in sandwich complexes usually deviate from the mean planes of the respective ligands $\eta^{\mu}\text{-C}_n\text{H}_n$; whereby for $n < 5$ the C–H bonds are directed away from the metal, for $n = 5$ they approximately lie in the ring plane, and for $n \geq 6$ they are bent toward the central metal atom.^{10b} Interestingly, the $\text{C}_{\text{Cp}}-\text{B}$ bond in **3*** displays a slight inclination toward the vanadium atom (angle 6.3° , 0.174 \AA deviation of the B atom from the C_5 -ring plane). The $-\text{B}(\text{OH})_2$ group in **3*** and the trigonal C atom in α -ferrocenyl carbenium ions ($\eta^5\text{-C}_5\text{H}_5$) $\text{Fe}(\eta^5\text{-C}_5\text{H}_4\text{C}^+\text{R}_2)$ share the presence of an sp^2 -hybridized atom, which is prone to interact with the central metal. However, whereas α -metallocenyl carbenium ions feature strongly bent $\text{C}_{\text{Cp}}-\text{C}^+\text{H}_2$ bonds, angles of 23.6° , 40.3° , and 41.8° relative to the ring planes having been reported for α -ferrocenyl-, ruthenocenyl-, and osmocenyl-carbenium ions,¹¹ this effect is not paralleled in magnitude by trovacenyl boronic acid. Presumably, the Lewis acidity of the boron center in **3*** is attenuated considerably by $\text{O} \rightarrow \text{B}$ donation as inferred from the B,O bond lengths of 1.35 and 1.37 \AA , which lie between those of a single and a double bond. The crystal

(10) (a) Engebretson, G.; Rundle, R. E. *J. Am. Chem. Soc.* **1963**, *85*, 481. (b) Lyssenko, K. A.; Antipin, M. Yu.; Ketkov, S. Yu. *Russ. Chem. Bull., Int. Ed.* **2001**, *50*, 130.

(11) Kreindlin, A. Z.; Dolgushin, F. M.; Yanovsky, A. I.; Kerzina, Z. A.; Petrovskii, P. V.; Rybinskaya, M. I. *J. Organomet. Chem.* **2000**, *616*, 106.

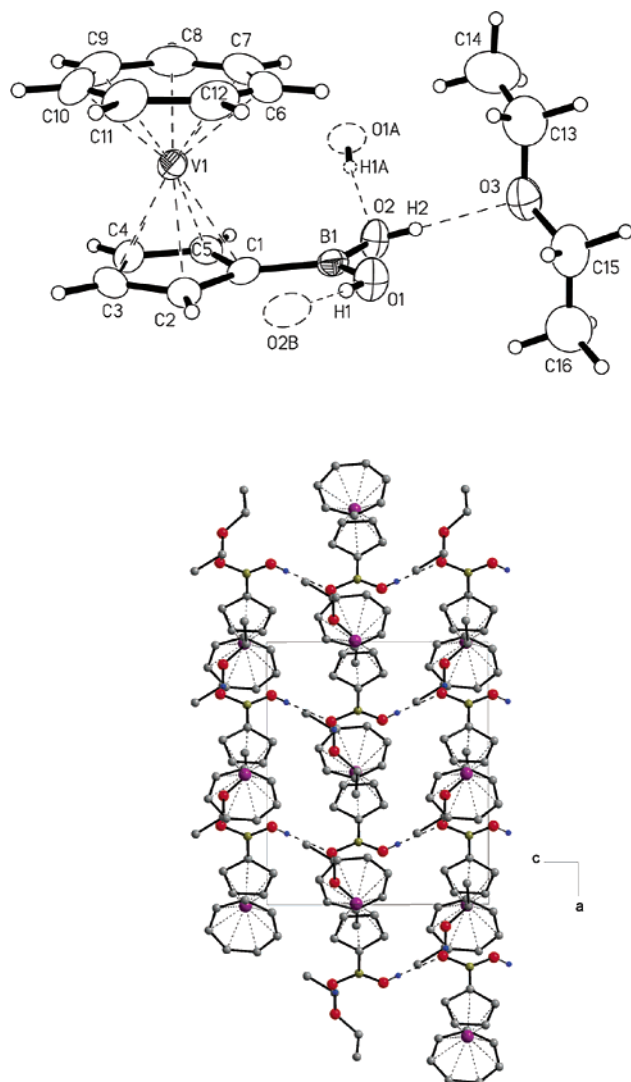


Figure 1. Structure of $3 \cdot \text{Et}_2\text{O}$ in the crystal. (a) Atomic labeling and view of a single unit in the direction of the strings ($\cdots\text{O}_\text{H}-\text{B}-\text{O}-\text{H}\cdots$)_n. (b) View perpendicular to the strings, depicting the alternating orientations of the trovaceny units attached to the strings. The axes of consecutive sandwich units assume 90° angles. Selected bond distances (Å): C–C (Cp, mean), 1.413(7); C–C (Tr, mean), 1.400(9); V(1)–C₅ (mean), 225.9; V(1)–C₇ (mean), 217.5; V(1)–C₅ (centroid), 191.3; V(1)–C₇ (centroid), 146.1; C(1)–B, 156.7(5); B–O(1), 134.7(7); B–O(2), 137.3(7); O(1)–H(1), 0.77(4); H(1)⋯O(2), 2.23(4); O(1)–H(1)⋯O(2), 2.988(4), angle $168(4)^\circ$; O(2)–H(2), 0.79(4); H(2)⋯O(3), 2.00(4); O(2)–H(2)⋯O(3), 2.781(4), angle $169(4)^\circ$.

structure of $3 \cdot \text{Et}_2\text{O}$, which contains infinite hydrogen-bonded chains ($\cdots\text{O}_\text{H}-\text{B}-\text{O}-\text{H}\cdots$)_n with suspended trovaceny units, resembles that of [5]trovacenol, ($\eta^7\text{-C}_7\text{H}_7$)V($\eta^5\text{-C}_5\text{H}_4\text{OH}$) (**9**).¹² In the case of **9** the strings ($\cdots\text{H}-\text{O}\cdots\text{H}-\text{O}\cdots$)_n place the trovaceny units in closer proximity and $\text{C}_7\text{H}_6-\text{H}\cdots\pi(\text{C}_5\text{H}_5)$ interactions between neighboring trovaceny groups constitute an additional bonding motif within the chains.

In crystals of the hydrate $3 \cdot \text{H}_2\text{O}$, the water molecule assumes the dual role of a donor and an acceptor, effecting coordination number four of the oxygen atom, just like in crystals of ice,¹³ as well as for internal water

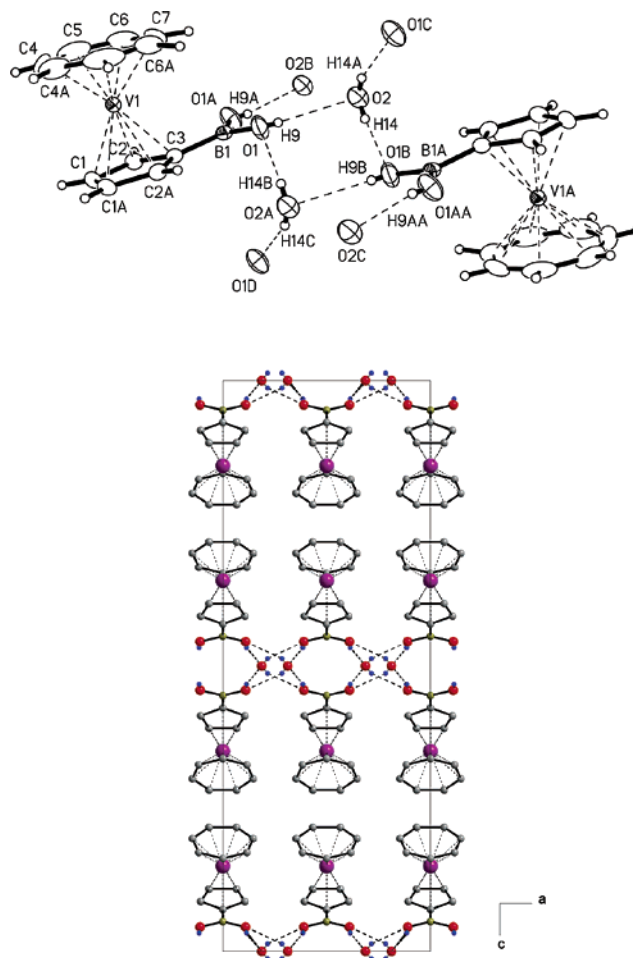


Figure 2. Structure of $3 \cdot \text{H}_2\text{O}$ in the crystal. (a) Numbering scheme and view of a pair of [5]trovaceny boronic acid molecules linked by indirect hydrogen bonding. (b) Strands of 12-membered rings (each composed of two $-\text{B}(\text{OH})_2$ groups and two H_2O molecules) which are interconnected by means of hydrogen bonding involving the water molecules. The suspended trovaceny units on both sides of the strand form rows of parallel units, and the angle between sandwich axes on opposite sides of the strand amounts to 180° , i.e., the unit cell of $3 \cdot \text{H}_2\text{O}$ possesses a center of inversion. Selected bond distances (Å): C–C (Cp, mean), 1.420(6); C–C (Tr, mean), 1.391(7); V(1)–C₅ (mean), 2.262; V(1)–C₇ (mean), 2.175; C(3)–B, 1.547(6); B–O(1), 1.355(3); O(1)–H(9), 0.57(3); H(9)⋯O(2), 2.25(4); O(1)–H(9)⋯O(2), 2.794(3), angle $162(6)^\circ$; O(2)–H(14), 0.58(4); H(14)⋯O(1), 2.314; O(2)–H(14)⋯O(1), 2.854(4), angle $158(7)^\circ$.

molecules in carbohydrates and proteins.¹⁴ The oxygen atoms of the $-\text{B}(\text{OH})_2$ groups are three-coordinate; however, they engage in B,O, donor, and acceptor hydrogen bonding. Contrary to $3 \cdot \text{Et}_2\text{O}$, in $3 \cdot \text{H}_2\text{O}$ both OH functions of the $-\text{B}(\text{OH})_2$ groups contribute to supramolecular organization, albeit indirectly in that they are separated by water molecules (Figure 2). The structure of $3 \cdot \text{H}_2\text{O}$ in the crystal may be described as a strand of 12-membered rings, the latter complying to the graph-set assignment $\text{R}_4^4(12)$ according to Etter.¹⁵ In these rings, the water molecules serve as hydrogen

(13) Savage, H. F. J.; Finney, L. J. *Nature* **1986**, 322, 717.

(14) Steiner, T.; Saenger, W. *J. Am. Chem. Soc.* **1993**, 115, 4540.
(b) Jeffrey, G. A. *An Introduction to Hydrogen Bonding*; Oxford University Press: New York, 1997.

(15) Etter, M. C. *Acc. Chem. Res.* **1990**, 23, 120.

(12) Elschenbroich, Ch.; Lu, F.; Harms, K. *Organometallics* **2002**, 21, 5152.

bond acceptors and the boryl groups as donors. The [5]-trovacenyl groups are connected to these rings in a trans orientation. The two water molecules of the $(\mathbf{3} \cdot \text{H}_2\text{O})_2$ units serve as hydrogen bond donors to neighboring units $(\mathbf{3} \cdot \text{H}_2\text{O})_2$, in this way generating the backbone of the strand. Since Brønsted acidity of boronic acids surpasses that of water (W), intra-ring hydrogen bonding (B)O–H \cdots O(W) [O \cdots O = 280 pm] is stronger than inter-ring hydrogen bonding (W)O–H \cdots O(W) [O \cdots O = 290 pm]. The structural comparison of the solvates $\mathbf{3} \cdot \text{Et}_2\text{O}$ and $\mathbf{3} \cdot \text{H}_2\text{O}$ once more illustrates the pronounced influence that the drive to satisfy all hydrogen-bonding capabilities may exert on crystal architecture.

Attempts to grow crystals of tri([5]trovacenyl)boroxine $\mathbf{4}^{\bullet\bullet}$ were frustrated by the low solubility in all common solvents. Yet it may be safely assumed that $\mathbf{4}^{\bullet\bullet}$, in the solid state, adopts the conformation given in Scheme 1, which is analogous to that in tri(ferrocenyl)boroxine, $\text{Fc}_3\text{B}_3\text{O}_3$ (**10a**),¹⁶ tri(ferrocenyl)boraselenine, $\text{Fc}_3\text{B}_3\text{Se}$ (**10b**),¹⁷ tri(ferrocenyl)borazine, $\text{Fc}_3\text{B}_3\text{N}_3$ (**10c**),¹⁶ and 1,3-di([5]trovacenyl)benzene (**11 \bullet**).¹⁸

Here, packing effects enforce conformations in which the η^5 -cyclopentadienyl rings of the [5]trovacenyl groups and the arene ring of the spacer are coplanar despite considerable *ortho*-hydrogen compression strain.

In fluid solution, however, conformations of $\mathbf{4}^{\bullet\bullet}$, in which the sandwich units are twisted with regard to the central boroxine ring, should be favored. This dichotomy is a general feature of trovacene derivatives to the effect that results from EPR spectroscopy (fluid solution) and magnetic susceptometry (solid state) may not be strictly comparable (vide infra).

Redox Properties. Studies of oligonuclear trovacene derivatives are of interest in the context of intermetallic electrocommunication. In the case of trovacenyl boranes, uncertainty as to the site of reduction, boron or vanadium, is a complicating factor.⁶ For the trovacenyl boronic acid $\mathbf{3}^{\bullet}$, discharge of acidic protons of the $-\text{B}(\text{OH})_2$ substituent may also contribute to cathodic currents. Both the trovacenyl boronic acid $\mathbf{3}^{\bullet}$ and the cyclic boronic ester $\mathbf{5}^{\bullet}$ in the (+/0) processes show small anodic shifts relative to parent $\mathbf{1}^{\bullet}$ amounting to +50 mV for $\mathbf{3}^{\bullet}$ and +53 mV for $\mathbf{5}^{\bullet}$. Thus, the $-\text{B}(\text{OH})_2$ group is only weakly electron withdrawing. Peak separation ΔE_p in the waves for the (+/0) processes is 90 mV. In the cathodic regime, irreversible reduction is observed for the boronic acid with a cathodic peak potential $E_{pc} = -2.86$ V. Reversible reduction occurs for the cyclic boronic ester $\mathbf{5}^{\bullet}$ at $E_{1/2}(0/-) = -2.44$ V, shifted anodically by +100 mV relative to parent $\mathbf{1}^{\bullet}$. Sufficient concentration for an electrochemical study of tri([5]trovacenyl)boroxine $\mathbf{4}^{\bullet\bullet}$ could only be achieved in the solvent dimethylformamide. As for the mononuclear complexes $\mathbf{3}^{\bullet}$ and $\mathbf{5}^{\bullet}$, oxidation of trinuclear $\mathbf{4}^{\bullet\bullet}$, relative to parent $\mathbf{1}^{\bullet}$, displays a small anodic shift of +50 mV. The wave for the oxidation of $\mathbf{4}^{\bullet\bullet}$ possesses a peak separation of 72 mV, no redox splittings $\delta E_{1/2}$, i.e., potential differences between subsequent redox steps, being resolved. To ascertain that this wave actually represents three

one-electron steps at nearly identical potential, di-(benzene)chromium (**8**) was added as an equimolar concentration standard. The peak currents for the waves at $E(\mathbf{8}^+/0) = -0.77$ V and $E(\mathbf{4}^{\bullet\bullet} 3+/2+, 2+/, +, 0) = +0.24$ V showed the expected 1:3 ratio. Therefore, as observed previously for triferrocenyl benzene (**12**)¹⁹ and di-, tri-, and tetra([5]trovacenyl)benzene derivatives,²⁰ intramolecular interactions between sandwich complexes as substituents at aromatic rings are too small to effect measurable shifts of the redox potentials for consecutive oxidation steps. Significantly larger mutual interactions are generally observed for reductions. However, in the case of $\mathbf{4}^{\bullet\bullet}$, due to the fact that reduction occurs close to the cathodic window of the medium, no reliable results could be obtained.

EPR Spectroscopy and Magnetism. Intermetallic communication in organometallic oligoradicals manifests itself in electron–electron spin–spin interaction, which can be quantified by determination of the exchange-coupling constant J .²¹ In the case of di- and trinuclear trovacene derivatives of the type reported here, this can be accomplished either by EPR spectroscopy, where the pertinent information is deduced from the ⁵¹V hyperfine pattern and its simulation, or by magnetic susceptometry via fitting the experimental data to the appropriate Bleaney–Bowers type formula. Eventual lack of correspondence between the results obtained from these methods derives from structural differences in solution and in the solid state and from weak intermolecular interactions present in solid samples.

Our motivation to prepare [5]trovacenyl boronic acid ($\mathbf{3}^{\bullet}$) also included the quest for a monomer \rightleftharpoons dimer equilibrium $2 \mathbf{3}^{\bullet} \rightleftharpoons (\mathbf{3}^{\bullet})_2$, effected by hydrogen bonding as observed for [5]trovacenyl carboxylic acid (**6**).⁵ Yet, even in meticulously dried aprotic organic solvents void of donor properties EPR spectroscopy pointed to the presence of the monomer $\mathbf{3}^{\bullet}$ only. Obviously, hydrogen bonding between $-\text{B}(\text{OH})_2$ groups is too weak to overrule the entropy factor that favors the monomers. Condensation to the cyclic anhydride tris([5]trovacenyl)boroxine ($\mathbf{4}^{\bullet\bullet}$) proceeds readily, however, affording $\mathbf{4}^{\bullet\bullet}$ upon heating in vacuo. This material possesses an extremely low solubility in all common solvents to the effect that EPR experiments always yielded superpositions of the spectra of the target compound $\mathbf{4}^{\bullet\bullet}$ and of a mononuclear trovacene derivative. It must be stressed that the composition of the solution does not represent

(16) Bats, J. W.; Ma, K.; Wagner, M. *Acta Crystallogr.* **2002**, C58, m129.

(17) Horn, H.; Rudolph, F.; Ahlrichs, R.; Merzweiler, K. *Z. Naturforsch.* **1992**, 47b, 1.

(18) Elschenbroich, Ch.; Wolf, M.; Schiemann, O.; Harms, K.; Burghaus, O.; Pebler, J. *Organometallics* **2002**, 21, 5810.

(19) (a) Kotz, J. C.; Painter, W. J. *J. Organomet. Chem.* **1971**, 32, 231. (b) Iyoda, M.; Kondo, T.; Okabe, T.; Matsuyama, H.; Sasaki, S.; Kuwatani, Y. *Chem. Lett.* **1997**, 35.

(20) (a) Schiemann, O.; Plackmeyer, J.; Fritscher, J.; Pebler, J.; Elschenbroich, Ch. *Appl. Magn. Reson.*, in press. (b) Schiemann, O. Ph.D. Thesis, Marburg, Germany, 1998.

(21) (a) Carlin, R. L. *Magnetochemistry*; Springer: Berlin, 1986. (b) Willet, R. D.; Gatteschi, D.; Kahn, O., Eds. *Magnetostructural Correlations in Exchange Coupled Systems*; Reidel: Dordrecht, 1985. (c) Kahn, O. *Molecular Magnetism*; VCH: Weinheim, 1993. (d) Bencini, A.; Gatteschi, D. *EPR of Exchange Coupled Systems*; Springer, Berlin, 1990. (e) Veciana, J., Ed. *π -Electron Magnetism. From Molecules to Magnetic Materials*; Springer: Berlin, 2001 (*Structure and Bonding*, 100). (f) Molin, Yu. N.; Salikov, K. M.; Zamaraev, K. I. *Spin Exchange, Principles and Applications in Chemistry and Biology*; Springer: Berlin, 1980. (g) McCleverty, J. A.; Ward, M. D. *Acc. Chem. Res.* **1998**, 31, 842. (h) Schäfer, K.-O.; Bittl, R.; Zweygart, W.; Lendzian, F.; Haselhorst, G.; Weyhermüller, T.; Wiegardt, K.; Lubitz, W. *J. Am. Chem. Soc.* **1998**, 120, 13104. (i) Crutchley, R. J. *Adv. Inorg. Chem.* **1994**, 41, 273. (j) Cano, J.; Ruiz, E.; Alvarez, S.; Verdager, M. *Comments Inorg. Chem.* **1998**, 20, 27.

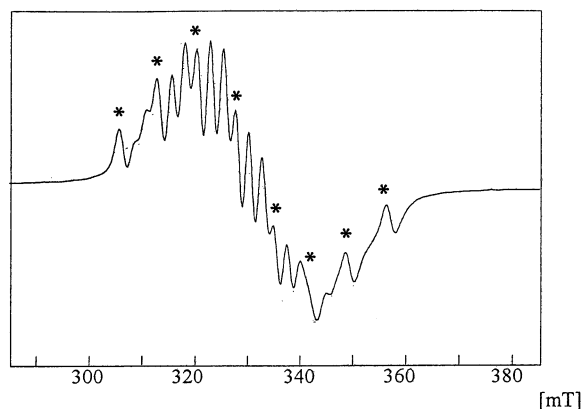


Figure 3. EPR spectrum (X-band, toluene, 295 K) of the triradical 1,3,5-tris([5]trovacenyl)boroxine (**4*****), ^{51}V hyperfine splitting 2.4 mT, superimposed on that of mononuclear [5]trovacenyl boronic acid, **3***, $a(^{51}\text{V}) = -7.24$ mT, $g = 1.983$. The latter is marked by asterisks; for line width effects see text.

that of the solid sample, which, according to mass spectrometry and elemental analysis, consists of practically pure **4*****. Rather, more soluble mononuclear **3*** is enriched in the saturated solution of sparingly soluble **4*****. As demonstrated in Figure 3, in addition to an octet of lines [$a(^{51}\text{V}, \mathbf{3}^*) = -7.24$ mT], indicative of a mononuclear trovacene derivative, a species with ^{51}V hyperfine splitting amounting to one-third of the coupling constant $a(^{51}\text{V}, \mathbf{3}^*)$ is present. This is characteristic for three interacting $^{51}\text{Vd}^5$ centers, engaged in exchange coupling for which $J \gg a(^{51}\text{V})$ holds. Not all of the expected 22 lines are seen because g and hyperfine anisotropies introduce an $m(^{51}\text{V})$ dependence of the line widths, outer lines being broadened more extensively than inner lines and high-field lines more than low-field lines.²²

The determination of a numerical value for the exchange coupling constant J of **4***** in fluid solution by simulation therefore must await retrieval of a higher quality spectrum. Visual inspection of the hyperfine pattern reveals, however, that $J(\mathbf{4}^{***})$ should resemble $J(\mathbf{7}^{**})$ for tris([5]trovacenyl)borane,⁶ and therefore the relation $J(\mathbf{4}^{***}) \approx 100a(^{51}\text{V})$ should hold [$a(^{51}\text{V}, \mathbf{1}^*) = 0.0057$ cm⁻¹]. Apparently, the larger extension of the bridge between two trovacenyl units in **4***** compared to **7**** is counterbalanced by smaller angles of twist of the trovacene axes in **4***** with concomitant superior conjugation.

Intramolecular exchange interaction in the triradical **4***** was also checked by means of magnetic susceptibility; the plot of χ^{-1} versus T is shown in Figure 4. The experimental data points were fitted to the expression for a triangular three-spin system given by Iwamura.²³ Since **4***** features a symmetrical equilateral structure, the choice $\alpha = 1$ was adopted for the parameter α , which accounts for disparate individual J values in cases of lower symmetry. The exchange coupling constant $J(\mathbf{4}^{***}) = -1.04$ cm⁻¹ was thus derived.²⁴ Most significantly, the exchange interaction turns out to be anti-

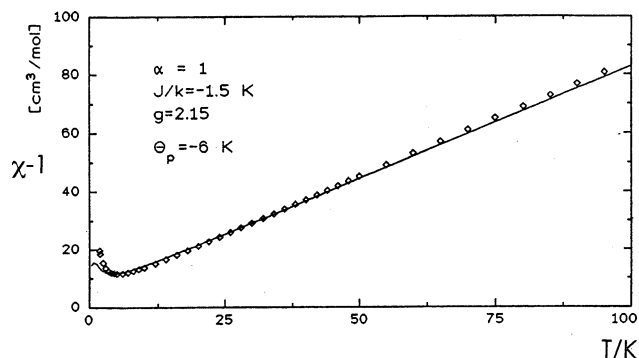


Figure 4. Temperature dependence of the inverse magnetic susceptibility (χ^{-1}) for tris([5]trovacenyl)boroxine, **4*****. The experimental data have been fitted by the equation given by Iwamura (ref 23).

ferromagnetic; thus, the triradical **4***** adds to the group of triradicals that possess a low-spin ground state despite the fact that a *meta*-phenylene type connectivity prevails for the spacer, in the case of **4***** the boroxine ring. It has been shown that in addition to bridging ligand topology (*o*-, *m*-, *p*-phenylene; 1,3,5-benzenetriyl, etc.) the extent of conjugation of the spin-bearing substituents with the transmitting unit, which is hampered by deviations from coplanarity, plays a decisive role.^{19,23,25} The lack of X-ray structure data for **4***** precludes a detailed discussion of the mechanism of antiferromagnetic exchange in solid **4*****.

The equilateral triangular disposition of the trovacenyl units and the antiferromagnetic nature of the interaction set the stage for spin frustration to operate in **4*****, however. Undoubtedly, the relatively small magnitude of $J(\mathbf{4}^{***})$ must be traced to this phenomenon. Comparatively small J values have previously been observed for the equilateral triangular triradicals tris([5]trovacenyl)borane (**7****)⁶ and 1,3,5-tri([5]trovacenyl)benzene.²⁰

It is gratifying to note that the magnitude of the exchange interaction determined in the solid state and the EPR features of **4***** in fluid solution concur. This is so because the values $|J(\mathbf{4}^{***})| = 1.04$ cm⁻¹ (magnetic susceptibility) and $|a(^{51}\text{V}, \mathbf{1}^*)| = 0.0057$ cm⁻¹ (EPR spectroscopy) imply $|J(\mathbf{4}^{***})| = 182 |a(^{51}\text{V}, \mathbf{1}^*)|$. Spectral simulations of exchange-coupled systems reveal that a multiplet structure composed of $2nI + 1$ components, separated by the intervals a/n , generally arises for $J \geq 10a$ (n = number of magnetic nuclei of spin I ; a = isotropic hyperfine coupling of the uncoupled monoradical).^{20b} Therefore, even if, because of less favorable conformations, exchange coupling for **4***** in solution is somewhat smaller than suggested by the value of J determined for solid **4*****, the gradation $J(\mathbf{4}^{***})_{\text{sol}} \gg$

(24) Optimal fit was achieved with the parameters $J/k_B = -1.5$ K, $\Theta = -6$ K, $g = 2.15$. The latter is somewhat surprising in view of the fact that for parent trovacene $g_{\text{iso}} = 1.987$ applies. However, since susceptibility was performed on a powder sample, g serves as a fitting parameter here which does not necessarily coincide with g_{iso} measured in fluid solution.

(25) (a) Rajca, A.; Lu, K.; Rajca, S.; Ross, C. R., II. *Chem. Commun.* **1999**, 1249. (b) Itoh, T.; Matsuda, K.; Iwamura, H. *Angew. Chem., Int. Ed.* **1999**, *38*, 1791. (c) Dvolaitzky, M.; Chiarelli, R.; Rassat, A. *Angew. Chem., Int. Ed. Engl.* **1992**, *31*, 180. (d) Francesconi, L. C.; Corbin, D. R.; Hendrickson, D. N.; Stucky, G. D. *Inorg. Chem.* **1979**, *18*, 3074. (e) Fieselman, B. F.; Hendrickson, D. F.; Stucky, G. D. *Inorg. Chem.* **1978**, *17*, 1841. (f) Ung, V. A.; Cargill Thompson, A. M. W.; Bardwell, D. A.; Gatteschi, D.; Jeffery, J. C.; McCleverty, J. A.; Totti, F.; Ward, M. D. *Inorg. Chem.* **1997**, *36*, 3447.

(22) Weil, J. A.; Bolton, J. R.; Wertz, J. E. *Electron Paramagnetic Resonance, Elementary Theory and Practical Applications*; Wiley: New York, 1994; p 321f.

(23) Fujita, J.; Tanaka, M.; Suemune, H.; Koga, N.; Matsuda, K.; Iwamura, H. *J. Am. Chem. Soc.* **1996**, *118*, 9347.

$a^{(51V, 1^*)}$ holds and the observation of a 22-line hyperfine structure with the splitting $a^{(51V)}/3$ meets expectation.

Experimental Section

Chemical manipulations and physical measurements were performed using standard techniques and instruments specified previously.⁶

[5]Trovacenyl Boronic Acid, (η^7 -C₇H₇)V[η^5 -C₅H₄B(OH)₂] (3^{*}). To a solution of trovacene (1^{*}, 0.60 g, 2.9 mmol) in 100 mL of diethyl ether was added at room temperature 4 mL of a solution (1.5 M) of *n*-butyllithium in hexane. After stirring for 14 h, a solution of freshly distilled tri-*n*-butylborate (1.61 mL, 6 mmol) in 100 mL of diethyl ether was added slowly at -78 °C. After 10 min the cooling bath was removed and stirring was continued for 20 h at room temperature. To the resulting dark red solution was added 100 mL of N₂-saturated aqueous HCl (6%). The organic phase was separated and extracted three times with 10% aqueous KOH solution. The blue aqueous phase, which contains the boronate (η^7 -C₇H₇)V-(η^5 -C₅H₄B(OH)₃)⁻, was carefully acidified with half-concentrated hydrochloric acid and subsequently extracted with one portion (100 mL) of benzene. The benzene layer was washed with water, dried with MgSO₄, and reduced in volume to effect precipitation of 3^{*} as a violet powder. Yield: 240 mg (33%). MS (EI, 70 eV): *m/z* (relative intensity) 699 ([M - H₂O]₃⁺, 8.2), 251 (M⁺, 100), 233 ([M - H₂O]⁺, 49.6), 142 (C₇H₇V⁺, 24.3). IR (KBr, cm⁻¹): 3371(s, b), 3040(w), 1800-1600(w), 1471(m), 1322(m), 1261(m), 783(s), 537(w), 434(w), 414(w). Anal. Calcd for C₁₂H₁₃BO₂V (255.99): C, 57.43; H, 5.22. Found: C, 56.99; H, 4.57.

Crystallization of Solvates of 3^{*}. Extraction with diethyl ether instead of benzene, reduction in volume, and cooling to 4 °C in a few days yields crystals of the solvate 3^{*}·Et₂O which are suitable for X-ray diffraction. If to the ether extract an aliquot of water is added and the two-phase system is stirred vigorously under vacuum to remove the diethyl ether, part of the product 3^{*} migrates to the aqueous phase. Stirring is stopped, and within a few hours crystals of the hydrate 3^{*}·H₂O form as 1–2 cm long violet needles.

2-[5]Trovacenyl-[1,3,2]-dioxaborolan (5^{*}). A solution of [5]trovacenyl boronic acid (3^{*}, 0.32 g, 1.28 mmol) and ethylene glycol (0.08 g, 1.28 mmol) in 10 mL of diethyl ether was refluxed for 3 h. Removal of the solvent in vacuo, dissolving the residue in toluene, and layering with *n*-pentane at 8 °C afforded violet cubes of 5^{*}. Yield: 0.40 g, 95%. MS (EI, 70 eV): *m/z* (relative intensity) 277 (M⁺, 100%), 142 (C₇H₇V⁺, 17.5%). Anal. Calcd for C₁₄H₁₅BO₂V (277.02): C, 60.70; H, 5.46. Found: C, 60.83; H, 5.25.

Tris([5]trovacenyl)boroxine (4^{*}).** [5]Trovacenyl boronic acid 3^{*} was suspended in benzene and refluxed for 10 m. After cooling to room temperature the benzene phase was decanted and the procedure was repeated twice. Filtration and drying in vacuo (3 × 10⁻³ mbar, 50 °C, 5 h) afforded the anhydride 4^{***} in quantitative yield as a pale violet powder which is practically insoluble in common organic solvents. MS (EI, 70 eV): *m/z* (relative intensity) 699 (M⁺, 100), 349 (M²⁺, 26.8), 233 ([M/3]⁺, 21.6), 142 (C₇H₇V⁺, 16.9). MS (high resolution): calcd for M⁺(¹²C) 699.10276, found 699.10412. Anal. Calcd for C₃₆H₃₃B₃O₃V₃ (698.91): C, 61.86; H, 4.76. Found: C, 61.67; H, 4.63.

X-ray Crystallographic Study of 3^{*}·Et₂O and 3^{*}·H₂O. Single crystals were mounted on a glass fiber in a drop of inert oil and frozen in the cold nitrogen stream of the cooling device.

Table 1. Summary of Crystal Structure Data for 3^{*}·Et₂O and 3^{*}·H₂O

	3 [*] ·Et ₂ O	3 [*] ·H ₂ O
empirical formula	C ₁₆ H ₂₃ BO ₃ V	C ₁₂ H ₁₅ BO ₃ V
fw	325.09	268.99
temperature (K)	223(2)	223(2)
cryst syst	orthorhombic	orthorhombic
space group	<i>Pca</i> 2 ₁	<i>Cmca</i>
<i>a</i> (Å)	11.9959(11)	10.730(2)
<i>b</i> (Å)	13.3325(14)	7.4100(10)
<i>c</i> (Å)	10.0958(8)	29.541(2)
<i>Z</i>	4	8
<i>V</i> (Å ³)	1614.7(3)	2348.8(6)
<i>D</i> _{calc} (Mg/m ³)	1.337	1.521
μ (mm ⁻¹)	0.620	0.835
<i>F</i> (000)	684	1112
cryst size (mm)	0.35 × 0.30 × 0.20	0.30 × 0.30 × 0.10
θ range (deg)	2.28–24.99	1.38–24.98
index ranges	<i>h</i> -14/14, <i>k</i> -15/15, <i>l</i> -12/12	<i>h</i> -1/12, <i>k</i> -1/8, <i>l</i> -35/1
no. of reflns collected	3041	1462
no. of indep reflns	2414	1093
	[<i>R</i> (int) = 0.0333]	[<i>R</i> (int) = 0.0329]
no. of obsd reflns	1897 [<i>I</i> > 2 σ (<i>I</i>)]	876 [<i>I</i> > 2 σ (<i>I</i>)]
no. of reflns used for refinement	2414	1093
treatment of hydrogen atoms	C-H calcd, O-H located and refined	located and refined isotropic refinement
extinction coeff		<i>X</i> = 0.0025(6)
Flack param	0.33(4) (racemic twin)	
largest diff peak and hole (e/Å ³)	0.208 and -0.244	0.488 and -0.612
no. of data/restraints/params	2414/1/200	1093/1/116
goodness-of-fit on <i>F</i> ²	1.028	1.010
wR2 (all data)	0.0966	0.1013
<i>R</i> 1 (obsd data)	0.0368	0.0397

The diffraction experiments were carried out at 213 K on a Siemens P4 four-circle diffractometer using graphite-monochromated Mo K α radiation. Cell parameters and orientation matrices for both complexes were obtained from least-squares refinement of 30 accurately centered high-angle reflections. No crystal decay was observed during the data collection. The structures were solved by direct methods.²⁶ Structure refinements were made on *F*² values by the full matrix least-squares technique.²⁷ The weighting scheme suggested by the program was used. All non hydrogen atoms were refined with anisotropic displacement parameters. A refinement of 3^{*}·Et₂O in the centrosymmetric space group *Pbcm* was not successful. Other experimental details and the crystal data are summarized in Table 1.

Acknowledgment. This work has been supported by the Volkswagen Foundation, the Deutsche Forschungsgemeinschaft, and the Fonds der Chemischen Industrie.

Supporting Information Available: Tables giving crystal data and details of the structure determinations, positional and thermal parameters, and all bond distances and angles for for 3^{*}·Et₂O and 3^{*}·H₂O. This material is available free of charge via the Internet at <http://pubs.acs.org>.

OM030574N

(26) Sheldrick, G. M. *SHELXS-97*, Program for the Solution of Crystal Structures; University of Göttingen: Germany, 1997.

(27) Sheldrick, G. M. *SHELXL-97*, Program for the Refinement of Crystal Structures; University of Göttingen: Germany, 1997.